THE JOURNAL OF BIOLOGICAL CHEMISTRY
Vol. 279, No. 16, Issue of April 16, pp. 15743–15751, 2004

Printed in U.S.A.

Subcellular Localization and Targeting of *N*-Acetylglucosaminyl Phosphatidylinositol De-*N*-acetylase, the Second Enzyme in the Glycosylphosphatidylinositol Biosynthetic Pathway*

Received for publication, December 10, 2003, and in revised form, January 22, 2004
Published, JBC Papers in Press, January 23, 2004, DOI 10.1074/jbc.M313537200

Anita Pottekat and Anant K. Menon‡
From the Department of Biochemistry, University of Wisconsin, Madison, Wisconsin 53706

The second step in glycosylphosphatidylinositol biosynthesis is the de-*N*-acetylation of *N*-acetylglucosaminylphosphatidylinositol (GlcNAc-PI) catalyzed by *N*-acetylglucosaminylphosphatidylinositol deacetylase (PIG-L). Previous studies of mouse thymoma cells showed that GlcNAc-PI de-*N*-acetylase activity is localized to the endoplasmic reticulum (ER) but enriched in a mitochondria-associated ER membrane (MAM) domain. Because PIG-L has no readily identifiable ER sorting determinants, we were interested in learning how PIG-L is localized to the ER and possibly enriched in MAM. We used HeLa cells transiently or stably expressing epitope-tagged PIG-L variants or chimeric constructs composed of elements of PIG-L fused to Tac antigen, a cell surface protein. We first analyzed the subcellular distribution of PIG-L and GlcNAc-PI-de-*N*-acetylase activity and then studied the localization of Tac-PIG-L chimeras to identify sequence elements in PIG-L responsible for its subcellular localization. We show that human PIG-L is a type I membrane protein with a large cytoplasmic domain and that, unlike the result with mouse thymoma cells, both PIG-L and GlcNAc-PI-de-*N*-acetylase activity are uniformly distributed between ER and MAM in HeLa cells. Analyses of a series of Tac-PIG-L chimeras indicated that PIG-L contains two ER localization signals, an independent retention signal located between residues 60 and 88 of its cytoplasmic domain and another weak signal in the luminal and transmembrane domains that functions autonomously in the presence of membrane proximal residues of the cytoplasmic domain that themselves lack any retention information. We conclude that PIG-L, like a number of other ER membrane proteins, is retained in the ER through a multi-component localization signal rather than a discrete sorting motif.

Glycosylphosphatidylinositol (GPI)[1] biosynthesis is initiated by transferring *N*-acetylglucosamine (GlcNAc) from UDP-GlcNAc to PI to generate *N*-acetylglucosaminylphosphatidylinositol (GlcNAc-PI). GlcNAc-PI is then de-*N*-acetylated and mannosylated. In mammalian cells and yeast, GlcN-PI must first be acylated on the inositol residue before mannose addition can occur. Mannosylated GPIs are substrates for phosphoethanolamine transferases that can add up to three phosphoethanolamine residues to the core glycan. GPIs containing a phosphoethanolamine cap may be enzymatically transferred to ER-translocated proteins with a C-terminal GPI signal sequence, thus generating a GPI-anchored protein destined for the cell surface (for review, see Refs. 1–4).

The GPI biosynthetic pathway is structurally, topologically, and spatially complex. It requires the participation of ~20 different gene products, some of which are organized as multi-subunit complexes (1, 4). Early biosynthetic steps occur on the cytoplasmic face of the ER, whereas later steps are located at the lumenal face (5, 6). This indicates that a GPI biosynthetic intermediate, likely GlcN-PI or GlcN-acyl PI, must flip across the ER membrane to be elaborated into a mature GPI structure (2, 7). Working with a mouse thymoma cell line (BW5147.3) we recently discovered that although the capacity to synthesize GlcNAc-PI appears to be uniformly distributed in the ER, the next five steps of GPI biosynthesis leading to the synthesis of the singly mannosylated GPI intermediate H5 (phosphoethanolamine-2Manα1–4GlcN-acyl-PI) is enriched in a domain of the ER that is associated with mitochondria (8). These mitochondria-associated ER membranes, or MAMs, correspond to a rapidly sedimenting ER fraction that is biochemically distinct from traditionally isolated endoplasmic reticula (9–11). The mechanisms involved in the biogenesis and maintenance of the MAM domain are unknown. Evidence for compartmentation of GPI biosynthetic enzymes within the ER was also reported in a different mouse thymoma cell line (EL4) using a gradient centrifugation approach to separate ER-derived membrane fractions (12).

The first of the MAM-enriched steps in the thymoma GPI biosynthetic pathway is the de-*N*-acetylation reaction that converts GlcNAc-PI to GlcN-PI (8). The reaction is catalyzed by PIG-L in mammals (Gpi12p in yeast) (1–4, 13, 14). Human PIG-L is a 252-amino acid membrane protein with a large cytoplasmic domain. Although PIG-L shows little homology to other known proteins, it contains a H*XX*EH zinc binding motif characteristic of many de-*N*-acetylases, and it specifically restores cell surface expression of GPI-anchored proteins in a GlcNAc-PI de-*N*-acetylase-defective Chinese hamster ovary (CHO) mutant cell line (15). Moreover, rat PIG-L protein, when expressed in and purified from *Escherichia coli*, possesses metal ion-dependent GlcNAc-PI de-*N*-acetylase activity (14). Studies using substrate analogues show that human and *Trypanosoma brucei* PIG-L differ significantly in their substrate

* This work was supported by National Institutes of Health Grant GM55427, Mizutani Foundation for Glycoscience Grant 020026 (both to A. K. M.), and a Mary Shine Peterson fellowship from the Department of Biochemistry, University of Wisconsin-Madison (to A. P.). The costs of publication of this article were defrayed in part by the payment of page charges. This article must therefore be hereby marked "*advertisement*" in accordance with 18 U.S.C. Section 1734 solely to indicate this fact.

‡ To whom correspondence should be addressed: Dept. of Biochemistry, University of Wisconsin, 433 Babcock Dr., Madison, WI 53706. Tel.: 608-262-2913; Fax: 608-262-3453; E-mail: menon@biochem.wisc.edu.

[1] The abbreviations used are: GPI, glycosylphosphatidylinositol; CHX, cycloheximide; ER, endoplasmic reticulum; FLAG epitope tag, 8-amino acid sequence consisting of DYKDDDDK; GFP, green fluorescent protein; GlcNAc, *N*-acetylglucosamine; GlcN, glucosamine; MAM, mitochondria-associated membrane; PIG-L, *N*-acetylglucosaminylphosphatidylinositol deacetylase; V5 epitope tag, 14-amino acid sequence consisting of GKPIPNPLLGLDST; PI, phosphatidylinositol; Endo H, endoglycosidase H; Mito, mitochondria; NST, *N*-glycosylation sequon; T-L-T, $Tac_{ecto}L_{1–26}Tac_{cyto}$; CHO, Chinese hamster ovary; PLAP, placental alkaline phosphatase; FACS, fluorescence-activated cell sorting; PBS, phosphate-buffered saline.

specificities, indicating that PIG-L may be an attractive target for the development of anti-parasite drugs (16–18).

We are interested in learning how PIG-L is localized to the ER and whether it contains signals or structural motifs that contribute to its presumed enrichment in the MAM. PIG-L, like other enzymes in the mammalian GPI biosynthetic pathway, has no readily identifiable sorting determinants such as the di-lysine or di-arginine motifs that have been shown to act as retrieval signals for certain ER membrane proteins (19). Thus, the mechanism by which PIG-L is localized to the ER is unclear. To address this issue, we analyzed PIG-L localization and targeting in HeLa cells, a cell type that has been used to assay inhibitors of PIG-L activity *in vitro* (16–18) as well as to study aspects of GPI biosynthesis (20, 21) and intracellular transport (22). We first carried out experiments to establish the subcellular distribution of PIG-L and GlcNAc-PI-de-*N*-acetylase activity in these cells using immunofluorescence microscopy and subcellular fractionation and then analyzed the subcellular distribution of various chimeric constructs to identify sequence elements in PIG-L responsible for its subcellular localization.

Our results show that although it is possible to generate a characteristic MAM fraction from HeLa cells, neither epitope-tagged PIG-L protein (transiently or stably expressed) nor GlcNAc-PI de-*N*-acetylase activity is enriched in this fraction. Instead, both PIG-L and GlcNAc-PI de-*N*-acetylase activity are uniformly concentrated in the ER and MAM. Thus, the sub-ER compartmentation of GPI synthesis observed previously in analyses of mouse thymoma cells (8, 12) appears not to be a feature of HeLa cells. We discuss this result in the context of precedents for cell type-specific differences in the fine subcellular distribution of a number of enzymes. To identify sequence elements in PIG-L responsible for its ER localization, we first established that PIG-L is a type I membrane protein and then analyzed the subcellular distribution of chimeric proteins consisting of PIG-L fragments fused to Tac antigen, a cell surface-expressed, *N*- and *O*-glycosylated type I membrane protein (23, 24). Using immunofluorescence microscopy and endoglycosidase treatment we analyzed the subcellular distribution of a series of transiently expressed chimeric proteins in which the Tac cytoplasmic tail and/or transmembrane domain were replaced with C-terminal truncation fragments of the PIG-L cytoplasmic domain. Our results show that the ER sorting information in human PIG-L is located in the cytoplasmic tail of the protein, with the sequence between residues 60 and 88 especially important. We also show that the PIG-L transmembrane span, although unable to act as an independent localization signal, can act in concert with severely truncated, non-functional cytoplasmic tail sequences to localize the corresponding chimeric constructs to the ER. We conclude that PIG-L, like a number of other ER membrane proteins, is retained in the ER through a multi-component localization signal rather than a discrete sorting motif.

EXPERIMENTAL PROCEDURES

Materials—Dulbecco's modified Eagle's medium, Ham's F-12 medium, fetal bovine serum, and penicillin/streptomycin were purchased from Invitrogen. Goat serum and cycloheximide were purchased from Sigma. Restriction enzymes, DNA modifying enzymes, and DNA polymerase were purchased from MBI Fermentas (Amherst, NY) and New England Biolabs (Beverly, MA). Protease inhibitor mixture and DNase I were purchased from Calbiochem and Amersham Biosciences, respectively. UDP-[^{3}H]GlcNAc (60 Ci/mmol) was from American Radiolabeled Chemicals (St. Louis, MO). Glass-backed silica 60 thin layer plates were from Merck.

Antibodies—Mouse monoclonal antibodies against FLAG and V5 epitope tags, green fluorescent protein (GFP), and human calnexin were purchased from Sigma, Invitrogen, MBL (Nagoya, Japan) and Transduction Laboratories (Lexington, KY), respectively. Mouse monoclonal anti-Tac antibodies 3G10 and anti-human placental alkaline phosphatase (PLAP) antibodies (clone 8B6) were purchased from Caltag Laboratories (Burlingame, CA) and DAKO (Carpinteria, CA), respectively. Rabbit polyclonal anti-V5 and anti-ribophorin I antibodies were kindly provided by Dr. Karen Colley (University of Illinois, Chicago, IL) and Dr. Christopher Nicchitta (Duke University Medical Center, Durham, NC), respectively. Rabbit polyclonal anti-Gpi8 antibodies were generated by Dr. Saulius Vainauskas in our laboratory using an *E. coli*-expressed polypeptide corresponding to residues 31–322 of human Gpi8. Horseradish peroxidase-conjugated anti-rabbit and anti-mouse antibodies were from Promega Corp. (Madison, WI). Goat anti-mouse and anti-rabbit IgGs conjugated with Alexa Fluor 568 or Alexa Fluor 488 were from Molecular Probes (Eugene, OR).

Plasmid Construction—Human PIG-L cDNA was obtained by PCR using a HeLa cell cDNA library as template (Invitrogen). To generate cDNA encoding N-terminal FLAG-tagged human PIG-L, a sense primer-containing sequence encoding a FLAG epitope tag (TGGAATTCCATCATGGACTACAAGGACGACGATGACAAGGAAGCAATGTGGCTCCTGTGT) was used in the PCR reaction in conjunction with an antisense primer (GAGGAAGCTTAGTGAGTTGATTCTCATGTAC). To generate cDNAs encoding FLAG-PIG-L-V5 and FLAG-PIG-L-GFP, the PCR fragment was cloned into a pEF6/V5 His vector (Invitrogen) using the TOPO cloning kit from Invitrogen or cloned into a pEGFPN1 vector (Clontech) using EcoRI and BamHI sites, respectively. An *N*-glycosylation site (ANSTS) was appended to the N terminus of FLAG-PIG-L-GFP using specific primers to obtain ANSTS-FLAG-PIG-L-GFP. Human Tac cDNA, a gift from Dr. Thomas Waldmann (NIH), was subcloned into pEF6/V5 His vector using BamHI and XbaI sites. Plasmids encoding chimeras of Tac and PIG-L were generated using PCR by the overlap extension method (25) and cloned into a pEF6/V5 His vector using BamHI and XbaI. Plasmid preparation and transformation were carried out according to standard protocols, and all constructs were verified by sequencing.

Cell Culture and cDNA Transfection—HeLa cells were cultured at 37 °C in a humidified 5% CO_2 atmosphere in Dulbecco's modified Eagle's medium supplemented with 10% (v/v) fetal bovine serum and penicillin/streptomycin. The CHO-K1 cell lines G9PLAP (stably expressing human placental alkaline phosphatase (PLAP) and its derivative G9PLAP 0.85 (a mutant lacking PIG-L protein (15)) were kindly provided by Dr. Victoria Stevens (Emory University School of Medicine, Atlanta, GA). CHO K1 cells were cultured in Ham's F-12 medium supplemented with 10% fetal bovine serum and penicillin/streptomycin. For transfections, exponentially growing cells were trypsinized and washed once with cytomix buffer (120 mM KCl, 0.15 mM $CaCl_2$, 25 mM Hepes/KOH, pH 7.6, 2 mM EGTA, 5 mM $MgCl_2$). The cells were resuspended at a density of 1×10^7 cells/ml in the same buffer, and 400 μl of suspension was transferred to a 0.4-cm electroporation cuvette (Invitrogen). 35 μg of DNA was added to the cell suspension in the cuvette and mixed well. The mixture was then exposed to a single electric pulse of 300 V with a capacitance of 1000 microfarads using an Invitrogen pulse system. The cells were allowed to recover in culture medium at 37 °C (5% CO_2 atmosphere) for 48 h before harvesting for biochemical analyses or immunofluorescence microscopy. HeLa cells stably expressing FLAG-PIG-L-GFP were selected by growing cells in 600 μg/ml G418 for 4 weeks and by subsequently maintaining the cultures in 250 μg/ml G418.

Flow Cytometric Analyses—G9PLAP 0.85 cells were transfected with 35 μg of vector DNA or epitope-tagged PIG-L constructs as described above. After ~48 h the cells were harvested and washed with fluorescence-activated cell sorting (FACS) buffer (phosphate-buffered saline (PBS) containing 5% fetal bovine serum, 0.1% sodium azide, 1 mM EDTA). The cells were stained with monoclonal anti-human PLAP (10 μg/ml) followed by 2 μg/ml phycoerythrin-conjugated goat anti-mouse secondary antibodies (Caltag Laboratories). Surface expression of PLAP was detected using a fluorescence-activated cell sorter (FACScan, BD Biosciences). Similar analyses were carried out with untransfected G9PLAP 0.85 or wild-type G9PLAP cells.

Fluorescence Microscopy—Transiently transfected HeLa cells were grown on coverslips for ~48 h in Dulbecco's modified Eagle's medium with 10% fetal bovine serum and penicillin/streptomycin. Cells were either treated with 100 μg/ml cycloheximide (CHX) for 2.5 h at 37 °C and then fixed or directly fixed with 4% paraformaldehyde for 15 min at ambient temperature. After three washes with ice-cold PBS, cells were either treated with digitonin (3 μg/ml in cytomix buffer with 0.3 M sucrose) for 30 min at 4 °C to selectively permeabilize the plasma membrane or with Triton X-100 (0.3% in PBS) for 25 min on ice to permeabilize all cellular membranes. For non-permeabilized samples, cells were left in cold PBS at 4 °C for 25 min. Permeabilized or non-permeabilized cells were then washed three times with PBS and incu-

bated with 10% goat serum albumin in PBS for 1 h. This was followed by incubation for 1 h at room temperature with anti-FLAG monoclonal antibody at 1 μg/ml, rabbit anti-V5 antibody at a 1:500 dilution, or anti-Tac monoclonal antibody at a 1:500 dilution. The cells were then washed with PBS three times and incubated with Alexa Fluor 568-conjugated goat anti-mouse IgG or goat Alexa Fluor 488-conjugated anti-rabbit IgG at a dilution of 1:500 for 1 h at room temperature. After four washes with PBS, the coverslips were mounted onto glass slides with a drop of Vectashield (Vector Laboratories, Burlingame, CA) and taken for confocal microscopy using a Bio-Rad confocal microscope (type MRC 1000).

Immunoprecipitation—Transfected HeLa cells (1–2 × 10^7) were scraped 2 days post-transfection, washed once with PBS, resuspended in 1 ml of MSB buffer (40 mM Hepes-KOH, pH 7.4, 150 mM NaCl, 0.5% (w/v) Nonidet P-40, and 1× protease inhibitor mixture (Calbiochem), and solubilized on ice for 30 min. The cell lysates were clarified by centrifugation at 10,000 × *g* for 20 min. The S10 supernatant thus obtained was further centrifuged at 100,000 × *g* for 45 min at 4 °C. To the supernatant fraction 30 μl of anti-FLAG M2-agarose (Sigma) slurry was added, and the sample was incubated at 4 °C overnight with gentle agitation. The agarose beads were pelleted by centrifugation (15 s, 10,000 × *g*) and washed 4 times with 1 ml of MSB buffer. Bound antigen was released by incubating the beads with FLAG peptide (250 μg/ml) in MSB buffer. For immunoprecipitation with anti-V5 or anti-Tac antibodies, the S10 supernatant was pre-cleared by incubating it with 20 μl of protein G-Sepharose resin slurry (Pierce) at 4 °C for 1 h. After a brief centrifugation (15 s, 10,000 × *g*) the supernatant was incubated with 1.5 μg of mouse monoclonal anti-V5 for 2 h at 4 °C. Protein G-Sepharose (20 μl of slurry) was then added, and the sample was incubated on a rotator at 4 °C overnight. The beads were pelleted, then washed 4 times with 1 ml of MSB buffer. Protein bound to the protein G-slurry was eluted by boiling in 1× denaturing buffer containing 0.5% SDS and 1% 2-mercaptoethanol for 5 min at 100 °C.

Glycosidase Treatment and Immunoblotting—cDNA corresponding to ANSTS-FLAG-PIG-L-GFP was electroporated into HeLa cells, and a lysate was prepared by resuspending cells in MSB buffer. The sample was denatured by adding 0.1 volume of 10× endoglycosidase H (Endo H) denaturation buffer (5% SDS, 10% 2-mercaptoethanol) and boiling for 5 min. Then 0.1 volume of 10× Endo H reaction buffer (0.5 M sodium citrate, pH 5.5) was added to the denatured sample followed by incubation with 250 units of Endo H for 2 h at 37 °C. Anti-V5 immunoprecipitates of Tac chimeras expressed in HeLa cells were similarly treated with Endo H. For peptide *N*-glycosidase F treatment of immunoprecipitated Tac chimeras, samples were eluted from antibody beads by boiling with 1× denaturation buffer, cooled to room temperature, and incubated with 0.1 volume of 10× peptide *N*-glycosidase F reaction buffer (0.5 M sodium phosphate, pH 7.5) containing 1% (w/v) Nonidet P-40. Samples were digested with 500 units of peptide *N*-glycosidase F for 2 h at 37 °C. After digestion, treated and untreated samples were boiled with SDS sample buffer containing 2-mercaptoethanol for 5 min. Treated and control samples were analyzed by SDS-PAGE and immunoblotting with mouse anti-GFP or rabbit anti-V5 antibodies. Immunoblots were visualized using ECL reagents from Pierce and quantitated using Image Quant software (Molecular Dynamics, Inc., Sunnyvale, CA).

Fractionation and GPI Assays—HeLa cells were grown on 12 × 150-mm plates to confluency. Cells from each plate (~1 × 10^7) were electroporated with 35 μg of DNA in a 0.4-cm cuvette and then re-plated to allow the cells to recover. Two days post-transfection cells were washed with PBS, resuspended in Buffer A (0.25 M sucrose, 10 mM Hepes/NaOH, pH 7.5, 1 mM dithiothreitol, and protease inhibitors) at a density of ~1 × 10^7 cells/ml and lysed by nitrogen bomb cavitation at 400 p.s.i. for 30 min on ice. Subcellular fractionation of lysed cells was carried out as previously described (8). Protein content of SDS-solubilized fractions was measured using the Micro-BCA protein assay reagent (Pierce). Samples for SDS-PAGE and immunoblot analysis were prepared by heating samples with SDS sample buffer for 1 h at 60 °C. Blot signals from different protein loadings and film exposure were quantitated using Image Quant software.

Fractions were characterized by measuring organelle-specific markers NADPH-cytochrome reductase *c* (ER marker) and succinate-cytochrome reductase *c* (inner membrane mitochondria marker). NADPH-cytochrome *c* reductase (ER marker) activity was measured spectrophotometrically by following the reduction of cytochrome *c* at 550 nm for 5 min. Different subcellular fractions were incubated in 1 ml of assay mixture containing 0.05 M phosphate buffer, 0.1 mM EDTA, pH 7.7, 36 μM cytochrome *c* at room temperature for 5 min with 2 μg/ml rotenone to inhibit the mitochondrion-specific NADH dehydrogenase. The reaction was initiated by adding 100 μl of 1 mM NADPH. Succinate-cytochrome *c* reductase, a mitochondrial inner membrane marker, was assayed as follows. Subcellular fractions were incubated with 1 ml of assay buffer containing 25 mM potassium phosphate, pH 7.2, 5 mM $MgCl_2$, 3 mM KCN, 20 mM succinate, and 2 μg/ml rotenone. The reaction was initiated by adding 39 μl of 1 mM cytochrome *c*, and the increase in absorbance was monitored for 5 min.

GlcNAc-PI de-*N*-acetylase activity was assayed by incubating subcellular fractions (10 μg) with [^{3}H]GlcNAc-PI (~2000 cpm) that had been previously solubilized in 0.1% Nonidet P-40 for 30 min at room temperature. Reactions were carried out at 37 °C in 200 μl of buffer containing 50 mM Hepes/NaOH, pH 7.4, 25 mM KCl, 5 mM $MgCl_2$, 5 mM $MnCl_2$, 0.5 mM dithiothreitol, 0.1 mM 1-chloro-3-tosylamido-7-amino-2-heptanone, and 1 μg/ml leupeptin. Reactions were stopped by placing the tubes on ice, and a single phase lipid extract was obtained by adding 160 μl of water, 40 μl of 1 N HCl, and 1.5 ml of ice-cold chloroform/methanol (v/v). A 2-phase mixture was induced by adding 0.5 ml of chloroform and 0.5 ml of water. The lipid-containing chloroform-rich lower phase was washed several times with 1.0 ml of mock upper phase, dried, and dissolved in water-saturated *n*-butyl alcohol. The radiolabeled lipids in the butanol extract were resolved by thin layer chromatography (silica gel 60; chloroform, methanol, 1 M ammonium hydroxide 10:10:3 (v/v/v)) and detected with a thin layer chromatography (TLC) radioscanner (Berthold Analytical Instruments, Inc. Nashua, NH). Incorporation of radioactivity into individual species ([^{3}H]GlcNAc-PI and [^{3}H]GlcN-PI) was determined using the integration software provided with the scanner. GlcNAc-PI de-*N*-acetylase activity was also measured indirectly by incubating isolated fractions (100 μg of protein) with UDP-[^{3}H]GlcNAc (1 μCi) in buffer A in the presence of 5 mM EDTA and 1 μg/ml PI dissolved in 0.1% Nonidet P-40 (total reaction volume, 200 μl). After 20 min of incubation at 37 °C samples were subjected to lipid extraction and analysis as described above.

RESULTS

Epitope-tagged PIG-L Constructs Are Functional—We generated several tagged versions of human PIG-L protein for use in the studies described in this paper. We determined that the tagged proteins were functional by testing their ability to restore cell surface expression of GPI-anchored PLAP in a GlcNAc-PI de-*N*-acetylase-deficient CHO-K1 mutant cell line (G9PLAP 0.85) (15). The mutant cells were transfected with plasmids encoding the tagged constructs, and cell surface expression of PLAP was assayed by FACS. Because PLAP is expressed at the cell surface only if it possesses a GPI anchor, the analysis is diagnostic for an intact GPI biosynthetic pathway. Inspection of the cell number density in the top left-hand quadrant (representing PLAP-positive live cells) of the FACS analysis panels in Fig. 1, *D–F*, indicates that the constructs FLAG-PIG-L-V5 and FLAG-PIG-L-GFP (with an N-terminal FLAG epitope tag and a V5 tag or GFP attached to the C terminus) as well as a chimera of Tac antigen and PIG-L (ΔTac-L_{26-252}; ΔTac fused to the cytoplasmic domain of PIG-L; see Fig. 4) were able to restore PLAP expression in the mutant cells (FACS data for wild-type and mutant cells are shown in Fig. 1A and B respectively). In contrast, transfection with vector DNA alone showed background levels of cell surface PLAP (Fig. 1*C*), comparable with that seen in the untransfected mutant cells (Fig. 1*B*). These data indicate that the various N-terminal and C-terminal tags do not affect the ability of PIG-L to restore GPI biosynthesis in a GlcNAc-PI de-*N*-acetylase-deficient cell line and that a significant fraction of the tagged PIG-L proteins is likely to be correctly localized within the cell.

Subcellular Distribution of PIG-L Protein; MAM Versus ER—To determine the subcellular distribution of GlcNAc-PI de-*N*-acetylase activity and PIG-L protein, HeLa cells expressing epitope-tagged PIG-L were homogenized by nitrogen cavitation and fractionated according to the scheme shown in Fig. 2*A*. Bulk ER membranes were recovered from the 10,000 × *g* supernatant (S10) after sucrose gradient centrifugation, whereas fractions corresponding to MAM and mitochondria (Mito) were derived from the 10,000 × *g* pellet (P10) (Fig. 2*A*).

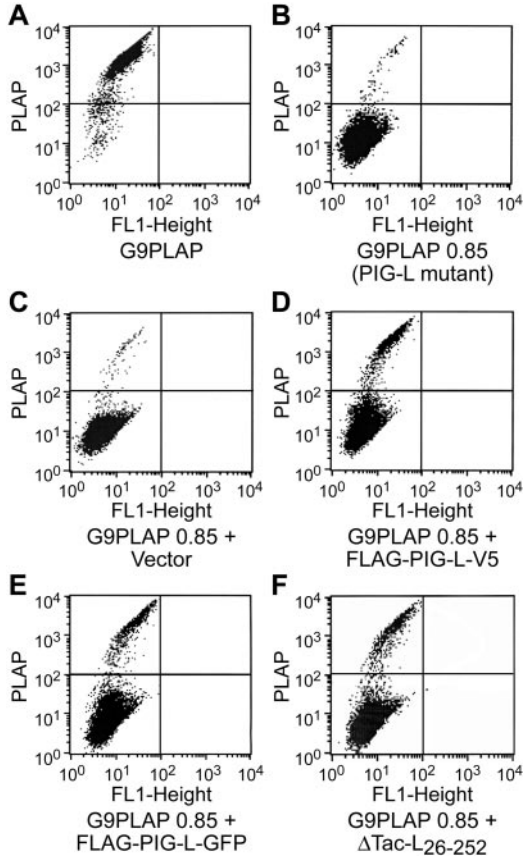

FIG. 1. **Epitope-tagged PIG-L constructs are functional.** The GlcNAc-PI de-*N*-acetylase-deficient CHO cell mutant, G9PLAP 0.85, was used to test the functionality of epitope-tagged PIG-L constructs. G9PLAP 0.85 cells, unlike the parental strain G9PLAP, are unable to express GPI-anchored PLAP at the cell surface. G9PLAP 0.85 cells were transfected either with an empty vector or plasmids encoding epitope-tagged PIG-L constructs (FLAG-PIG-L-V5, FLAG-PIG-L-GFP, or ΔTac-L_{26-252}). Two days post-transfection, the cells were analyzed by FACS for cell surface expression of PLAP. The top left quadrant in each of the FACS analyses demonstrates the surface expression of PLAP in G9PLAP cells (*A*), G9PLAP 0.85 cells (*B*), and G9PLAP 0.85 cells transfected with vector cDNA (*C*), FLAG-PIGL-V5 (*D*), FLAG-PIG-L-GFP (*E*), or ΔTac-L_{26-252} (*F*).

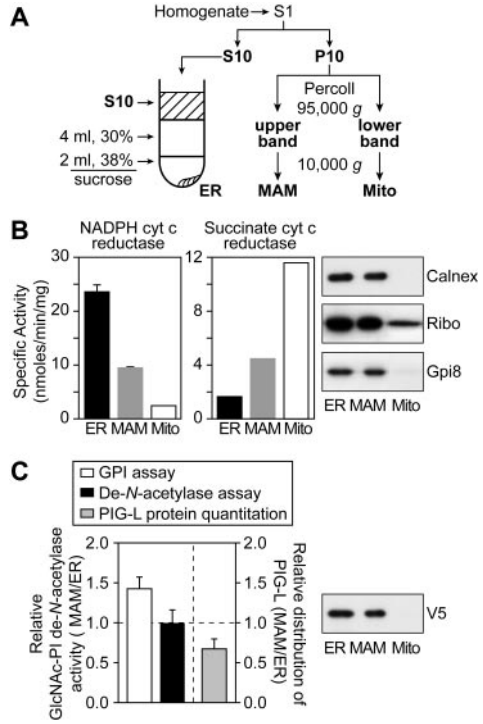

FIG. 2. **Subcellular distribution of GlcNAc-PI de-*N*-acetylase activity and epitope-tagged PIG-L.** *A*, schematic outline of the subcellular fractionation protocol used to isolate ER, MAM, and Mito fractions from a HeLa cell homogenate. Details are provided under "Experimental Procedures." *B*, specific activities of organelle specific markers in ER, MAM, and Mito fractions. The immunoblots represent equal protein loading. Data are averaged from two independent fractionation experiments using HeLa cells transiently expressing FLAG-PIG-L-V5. Protein recovered in each of the fractions was for ER (2.2 ± 0.2 mg), MAM (2.4 ± 0.2 mg), and Mito (1.8 ± 0.4 mg). Similar protein and marker distributions were obtained in fractionation experiments with wild-type (non-transfected) HeLa cells and with HeLa cells stably or transiently expressing FLAG-PIG-L-GFP. *C*, GlcNAc-PI de-*N*-acetylase activity was measured directly using exogenously added [^{3}H]GlcNAc-PI as substrate (*De-N-acetylase assay*) or indirectly using [^{3}H]GlcNAc-PI synthesized *in situ* from UDP-[^{3}H]GlcNAc and PI (*GPI assay*). The ratio of GlcNAc-PI de-*N*-acetylase activity in the MAM *versus* the ER is plotted for fractions derived from HeLa cells transiently expressing FLAG-PIG-L-V5. The GPI assay represents the average of two independent fractionation experiments. ER, MAM, and Mito fractions from HeLa cells transiently expressing FLAG-PIG-L-V5 were resolved by SDS-PAGE and immunoblotted with anti-V5 antibodies. Several different exposures of the blots were quantitated and normalized to the corresponding calnexin signal. The ratio-normalized signal in MAM *versus* ER is plotted. *cyt c*, cytochrome c; *Ribo*, ribophorin I.

The fractionation procedure shown in Fig. 2*A* has been extensively characterized for various mammalian cell types, including hepatocytes, CHO cells, and thymoma cells (8, 9, 26, 27). We therefore present only a brief characterization of the fractions to authenticate our procedures for HeLa cells. Fig. 2*B* shows that the specific activity of the ER marker NADPH cytochrome *c* reductase is characteristically ~2.5-fold lower in MAM compared with ER, whereas the concentration (per mg of protein) of the chaperone calnexin and the oligosaccharyltransferase subunit ribophorin I is similar in ER and MAM fractions (the overexposed blot for ribophorin I reveals a small amount of cross-contamination in the Mito fraction). Interestingly, the Gpi8 subunit of GPI transamidase, the enzyme responsible for GPI attachment to proteins (1–4), is also equally distributed between ER and MAM (Fig. 2*B*). The specific activity of the mitochondrion inner membrane marker succinate cytochrome *c* reductase was highest in the Mito fraction, as anticipated, and lowest in the ER. The MAM fraction displayed a slightly higher specific activity for succinate cytochrome *c* reductase activity than did the ER, probably because of the co-isolation of mitochondrial contact site membranes and, hence, some mitochondrial inner membrane with MAM. The marker enzyme pattern for the HeLa ER, MAM, and Mito fractions shown in Fig. 2*B* is similar to that described previously for other cell types (8, 9, 26).

To determine the subcellular distribution of PIG-L and specifically to test whether PIG-L protein was enriched in MAM relative to ER, we fractionated HeLa cells that had been transfected with cDNA encoding FLAG-PIG-L-V5. ER and MAM fractions were analyzed by SDS-PAGE and immunoblotting with anti-V5 antibodies to probe the distribution of FLAG-PIG-L-V5. The blots showed similar levels of FLAG-PIG-L-V5 in both ER and MAM, with no detectable signal in the Mito fraction (Fig. 2*C*). Densitometric comparison of the blot signals from different protein loadings and film exposures indicated that the ratio of the FLAG-PIG-L-V5 signal in the MAM *versus* ER was ~0.65 (Fig. 2C). These data clearly indicate that transiently expressed FLAG-PIG-L-V5 is not specifically enriched in the MAM and in the experiment shown appears to be somewhat depleted from the MAM fraction. Similar results were obtained in analyses of cells transiently or stably expressing FLAG-PIG-L-GFP (data not shown).

We were concerned that our results could have been influenced by protein overexpression, resulting in accumulation of PIG-L in the ER due to saturation of a putative MAM sorting machinery or slow folding of the protein. Although these concerns were somewhat mitigated by our results showing that stably transformed cell lines with a lower level of PIG-L expression yielded the same ER-MAM distribution pattern for PIG-L as cells transiently expressing the protein, we extended our experiments by analyzing PIG-L distribution in cells treated with CHX. We anticipated that the CHX-induced block in protein synthesis would effectively chase any unfolded PIG-L into folded form without increasing the level of expressed protein. The fractionation data we obtained from CHX-treated HeLa cells stably expressing FLAG-PIG-L-GFP were identical to our results with untreated cells, *i.e.* PIG-L was similarly concentrated in the ER and MAM fractions (data not shown). We conclude that our results are unlikely to have been influenced by protein overexpression.

In view of our unexpected data on the subcellular distribution of PIG-L we investigated the distribution of GlcNAc-PI de-*N*-acetylase activity in MAM and ER fractions from HeLa cells. Cells transiently expressing FLAG-PIG-L-V5 were fractionated as in Fig. 2*A*. The resulting MAM and ER fractions were incubated with [^{3}H]GlcNAc-PI at 37 °C for different periods of time, then processed by lipid extraction and TLC. The extent to which [^{3}H]GlcNAc-PI was converted to [^{3}H]GlcN-PI was determined after visualizing the chromatograms with a radioactivity scanner. The ratio of GlcNAc-PI de-*N*-acetylase activity in MAM relative to ER was ~1. Thus, the distribution of GlcNAc-PI de-*N*-acetylase activity in the two fractions roughly mimics that of the distribution of PIG-L protein (Fig. 2*C*; *de-N-acetylase assay*).

We also assayed GlcNAc-PI de-*N*-acetylase activity indirectly by incubating ER and MAM fractions with UDP-[^{3}H]GlcNAc and PI and measuring the yield of [^{3}H]GlcN-PI as a percentage of total radiolabeled lipid ([^{3}H]GlcNAc-PI + [^{3}H]GlcN-PI). Previous work (8), reinforced by our preliminary studies in HeLa membranes (not shown), showed that GlcNAc-PI de-*N*-acetylase activity correlates well with the indirect measure of activity provided by this assay. The relative percent yield of [^{3}H]GlcN-PI (MAM *versus* ER) obtained in this fashion was ~1.4 (Fig. 2*C*; GPI assay). Similar data were obtained using ER and MAM fractions derived from untransfected HeLa cells as well as from cells stably or transiently expressing epitope-tagged variants of PIG-L (not shown).

We conclude that GlcNAc-PI de-*N*-acetylase activity and PIG-L protein are similarly concentrated (per mg of protein) in ER and MAM fractions derived from HeLa cells. This result differs in detail from previous observations with mouse thymoma cell lines which indicated that although GlcNAc-PI de-*N*-acetylase activity is found in both ER and MAM, it is significantly enriched in MAM (8). The difference may be attributed to subtle, cell type-specific variation in subcellular compartmentation. For the purpose of identifying subcellular targeting signals as described below, we consider PIG-L to be an ER-localized protein in HeLa cells.

PIG-L Is a Type I Membrane Protein—To set up suitable constructs for analysis of ER targeting signals in PIG-L, we needed to establish the membrane topology of the protein. Previous protease protection experiments suggested that rat PIG-L is a bitopic membrane protein with a large C-terminal cytoplasmic domain and both its N and C termini oriented to the cytoplasm (13). However, hydropathy analyses indicate that human PIG-L has only one strongly predicted transmembrane span. To clarify this issue and determine the topology of human PIG-L, we took two approaches. First, HeLa cells were transfected with cDNA corresponding to FLAG-PIG-L-V5, then treated with digitonin (to selectively disrupt the plasma membrane) or Triton X-100 (to disrupt all membranes) before labeling the cells with antibodies to the FLAG or V5 epitope tags and visualizing the staining pattern by indirect immunofluorescence microscopy. The FLAG tag could not be visualized in digitonin-treated cells, whereas the V5 tag displayed a reticular staining pattern characteristic of the ER (Fig. 3*A*). This result suggests that the N-terminal FLAG tag is protected in the ER lumen and consequently inaccessible to antibodies in digitonin-permeabilized cells, whereas the C-terminal V5 tag is oriented toward the cytoplasm. Both tags could be visualized in Triton X-100-treated cells, where all membranes are disrupted. These results are consistent with a type I membrane protein topology.

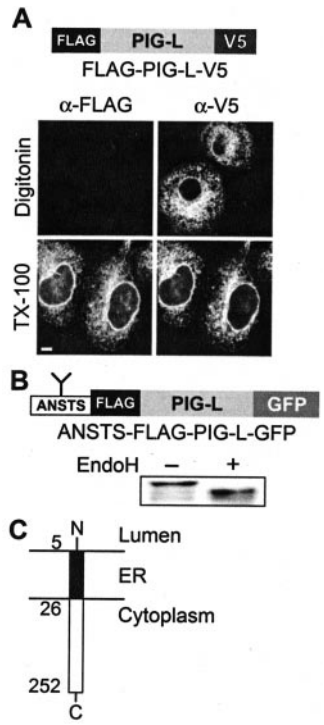

FIG. 3. **PIG-L is a type I ER membrane protein.** *A*, FLAG-PIG-L-V5 was transiently expressed in HeLa cells. The cells were fixed, then selectively permeabilized with either digitonin (*top panels*) or TX-100 (*lower panels*) and stained with anti-FLAG or anti-V5 antibodies. Bound primary antibodies were visualized using Alexa Fluor-conjugated secondary antibodies. The FLAG epitope was inaccessible after selective permeabilization of the plasma membrane with digitonin, indicating that the N terminus of PIG-L is oriented toward the ER lumen. The C-terminal V5 epitope was accessible after digitonin permeabilization, indicating that the C terminus of the protein faces the cytoplasm. *Scale bar*, 5 μm. *B*, an *N*-glycosylation sequon (Asn-Ser-Thr) was appended to the N terminus of FLAG-PIG-L-GFP to generate the construct ANSTS-FLAG-PIG-L-GFP. Cell lysates from HeLa cells expressing this construct were either treated with Endo H or mock-untreated, then analyzed by 8% SDS-PAGE and immunoblotting with anti-GFP antibodies. A specific band with a molecular mass corresponding to the size of ANSTS-FLAG-PIG-L-GFP (~60 kDa; also detected by anti-FLAG antibodies) was seen to be sensitive to Endo H, confirming the luminal orientation of the N-terminal ANSTS sequence. *C*, schematic of PIG-L topology based on hydropathy analyses and data shown in *panels A* and *B*.

In a second approach to determine the membrane topology of PIG-L, we analyzed the glycosylation status of a PIG-L construct (ANSTS-FLAG-PIG-L-GFP) in which we introduced an *N*-glycosylation sequon (NST) N-terminal to the FLAG tag (there are no *N*-glycosylation sites in native human PIG-L). When expressed in HeLa cells, this construct was seen to be modified by an endoglycosidase H-sensitive *N*-glycan, estab-

lishing that the N terminus of the protein was located in the ER lumen, where it could be accessed by oligosaccharyltransferase (Fig. 3*B*). We note that the Endo H sensitivity of the glycosylated construct is consistent with its ER localization.

The experimental evidence presented above together with hydropathy predictions suggests that human PIG-L is a type I membrane protein. Based on hydropathy predictions we suggest that PIG-L has a very short N-terminal sequence projecting into the ER lumen (amino acids 1–5), a transmembrane span (amino acids 6–25), and a large cytoplasmic C-terminal domain (amino acids 26–252) (Fig. 3*C*).

The Cytoplasmic Domain of PIG-L Contains an ER Localization Signal—In the experiment described in Fig. 3*B*, we noted that the *N*-glycan added to ANSTS-FLAG-PIG-L-GFP is sensitive to Endo H, indicating that the ANSTS-FLAG-PIG-L-GFP protein is confined to the ER and does not get detectably exposed to *N*-glycan-modifying medial Golgi enzymes. This result suggests that PIG-L is localized to the ER by a direct retention mechanism rather than by detectable cycles of escape and retrieval. To identify an ER retention signal in PIG-L, we analyzed the subcellular distribution of chimeric proteins composed of elements of PIG-L fused to Tac antigen, the α-subunit of the interleukin 2 receptor (23, 24). Tac is a type I plasma membrane protein of 251 amino acids with a large ectodomain, a single membrane-spanning domain, and a short 13-amino acid cytoplasmic tail (Fig. 4*A*). Tac lacks any intrinsic ER retention or retrieval signals and possesses two *N*-glycosylation sequons and a number of potential *O*-glycosylation sites in its ectodomain that can be used to assess its location in the secretory pathway. Our approach was to identify PIG-L sequences, which when fused to Tac, would cause Tac to be retained in the ER rather than be exported to the cell surface.

HeLa cells were transfected with cDNA corresponding to Tac with a C-terminal V5 epitope tag, and the distribution of the protein was visualized by antibody staining of intact cells as well as Triton X-100-permeabilized cells. As shown in Fig. 4*B*, Tac was strongly labeled in intact cells, consistent with its cell surface localization. A truncation construct, ΔTac, lacking the cytoplasmic tail of Tac antigen also showed clear surface staining in intact cells, although there appeared to be more intracellular staining possibly due to slower exit from the ER. This result confirms that the loss of the cytoplasmic domain does not retain Tac in the ER. In contrast, a chimeric construct (Tac_{ecto}-L) consisting of the ecto domain of Tac fused to PIG-L showed a clear ER reticular staining pattern in permeabilized cells and essentially no staining in intact cells (Fig. 4*B*). A chimeric protein (ΔTac-L_{26-252}) composed of ΔTac fused to the cytoplasmic portion of PIG-L (residues 26–252) was also ER-localized (Fig. 4*B*). To demonstrate that ER localization of this construct was not a result of slowed export, cells were chased for 2.5 h in the presence of CHX to block new protein synthesis. Under these conditions ΔTac-L_{26-252} was still localized to the ER. Consistent with its ER localization we showed that ΔTac-L_{26-252} was functional by demonstrating its ability to restore surface expression of PLAP in G9PLAP0.85 GlcNAc-PI-de-*N*-acetylase-deficient cells (Fig. 1*F*).

We confirmed the subcellular distribution of the various constructs by immunoprecipitating the proteins from cell lysates and analyzing them by endoglycosidase treatment and SDS-PAGE. SDS-PAGE analysis of the Tac and ΔTac samples indicated two forms of each of the proteins, running roughly with the ~50- and ~64-kDa molecular mass markers. The lower molecular mass form in each case is likely a precursor located in the early secretory pathway since it has Endo H- and peptide *N*-glycosidase F-sensitive *N*-glycans, whereas the dominant higher molecular mass form in each case likely corresponds to the cell surface form

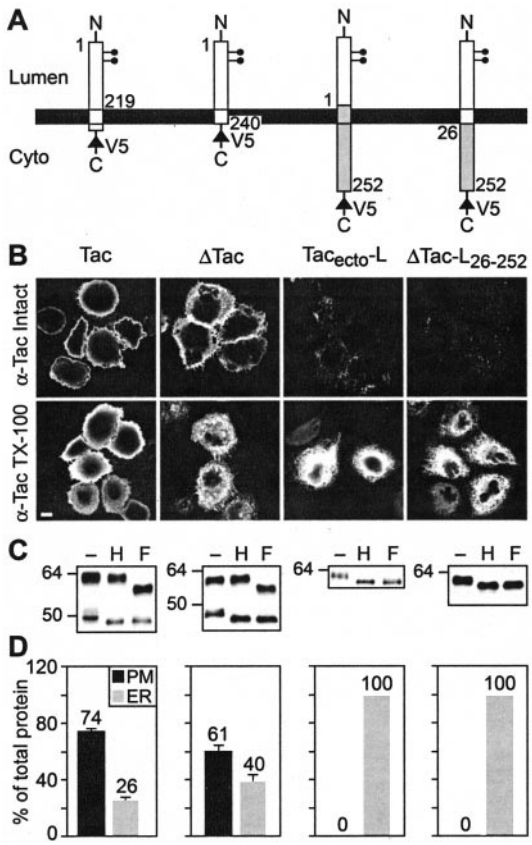

FIG. 4. **PIG-L contains ER retention information.** *A*, schematic illustration of Tac, ΔTac, and Tac-PIG-L fusion proteins (Tac_{ecto}-L and ΔTac-L_{26-252}). *N*-glycosylation sites in the Tac ecto domain are indicated by the *filled circles*; Tac is also *O*-glycosylated (not shown). All constructs have a C-terminal V5 epitope tag, indicated by the f*illed triangle*. *Cyto*, cytoplasm. *B*, HeLa cells were transfected with cDNAs encoding Tac, ΔTac, Tac_{ecto}-L, or ΔTac-L_{26-252}. Two days post-transfection, the cells were fixed (*Intact*) or fixed and permeabilized (*TX-100*), then labeled with antibodies to Tac antigen. The subcellular distribution of the constructs was visualized by confocal fluorescence microscopy after staining with fluorescence-conjugated secondary antibodies. Staining with anti-V5 antibodies co-localized with that seen with anti-Tac antibodies in permeabilized cells. *Scale bar*, 5 μm. *C*, HeLa cells transfected with cDNAs encoding Tac, ΔTac, Tac_{ecto}-L, or ΔTac-L_{26-252} were lysed 2 days post-transfection, and the expressed proteins were immunoprecipitated with monoclonal anti-V5 antibodies. Equal amounts of samples (~30% of the total) were digested with Endo H (*H*) or peptide *N*-glycosidase F (*F*), resolved on 8% SDS-PAGE along with untreated samples, and immunoblotted with rabbit anti-V5 antibodies. Both Tac and ΔTac show Endo H-sensitive and -resistant forms, whereas Tac_{ecto}-L or ΔTac-L_{26-252} show only a single Endo H-sensitive form. *D*, different exposures of the blots shown in *panel C* were quantitated using Image Quant software. The percentage of cell surface (Endo H-resistant, high molecular mass) and ER form (Endo H-sensitive, low molecular mass) for each construct is shown. *PM*, plasma membrane.

of the protein since it displays Endo H-resistant, peptide *N*-glycosidase F-sensitive, Golgi-modified *N*-glycans (Fig. 4*C*). The considerable difference in molecular mass between the two forms is due to *O*-glycosylation, confirming the post-ER localization (28) of the higher molecular mass form. In contrast to the results with Tac and ΔTac, analyses of both Tac_{ecto}-L and ΔTac-L_{26-252} revealed only a single, Endo H-sensitive polypeptide (Fig. 4*C*), consistent with the ER localization established by immunofluorescence microscopy.

Fig. 4*D* provides a quantitative assessment of the relative amounts of Endo H-sensitive (ER) *versus* Endo H-resistant (plasma membrane) form of each protein. These data indicate that the cytoplasmic domain of PIG-L contains ER localization information capable of retaining Tac fusion proteins in the ER.

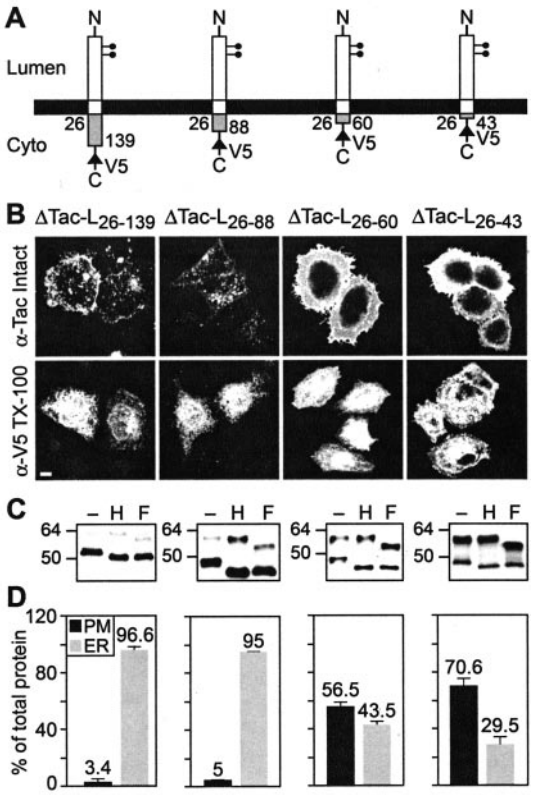

FIG. 5. **The cytoplasmic domain of PIG-L contains an ER retention signal.** *A*, schematic illustration of a series of chimeric constructs (ΔTac-L_{26-139} through ΔTac-L_{26-43}) derived from ΔTac-L_{26-252} (Fig. 4*A*). All constructs contain a C-terminal V5 tag. *Cyto*, cytoplasm. *B*, HeLa cells were transfected with cDNAs encoding the various constructs, then processed as described in the legend to Fig. 4*B* except that intact cells were stained with anti-Tac antibodies, and permeabilized cells were stained with anti-V5 antibodies. *Scale bar*, 5 μm. *C*, the expressed proteins were immunoprecipitated from cell lysates and analyzed by glycosidase digestion and SDS-PAGE as described in the legend to Fig. 4*C*. *H*, Endo H; *F*, *N*-glycosidase F. *D*, quantitation of the immunoblots in *panel C* was carried out as described in the legend to Fig. 4*D*. *PM*, plasma membrane.

ER-targeting Information in PIG-L Localizes to a Region between Amino Acids 60 and 88—To define regions within the cytoplasmic domain of PIG-L that are responsible for its ER localization, we analyzed a series of chimeric constructs (ΔTac-L_{26-139}, ΔTac-L_{26-100}, ΔTac-L_{26-88}, ΔTac-L_{26-60}, and ΔTac-L_{26-43} (Fig. 5*A*; ΔTac-L_{26-100} is not shown)) derived from ΔTac-L_{26-252} (Fig. 4*A*) in which the cytoplasmic tail of PIG-L was progressively truncated from the C terminus. All deletions were made at junctions between predicted structural domains to minimize the perturbing influence of the truncations on the folding of the expressed proteins. We expressed the constructs in HeLa cells and analyzed their subcellular distribution by immunofluorescence microscopy and glycosidase digestion.

Deletion of 113 amino acids from the C terminus of PIG-L (construct ΔTac-L_{26-139}) yielded an Endo-H-sensitive chimeric protein that was predominantly localized to the ER even after a 2.5-h CHX chase (Fig. 5, *B* and *C*; data not shown for the CHX chase). However, the construct displayed a low level of surface expression (<5%; as judged by the yield of the high molecular mass, Endo-H-resistant form of the chimera (Fig. 5, *C* and *D*)), suggesting that deletion of 113 amino acids from the C-terminus of PIG-L allowed for low efficiency exit from the ER.

As shown in Fig. 5*B*, progressive C-terminal truncations led to a sharp change from ER localization to plasma membrane localization once more than 164 amino acids had been deleted. Constructs ΔTac-L_{26-100} (not shown) and ΔTac-L_{26-88} resembled ΔTac-L_{26-139} in being predominantly ER-localized, as judged by immunofluorescence microscopy as well by glycosidase digestion and SDS-PAGE analysis. However, further truncations yielded chimeras that were clearly exported to the cell surface, as visualized by staining of intact cells with anti-Tac antibodies (Fig. 5*B*). Consistent with this, ~55% of ΔTac-L_{26-60} and ~70% of ΔTac-L_{26-43} were recovered as high molecular mass products with Endo H-resistant glycans. These results suggest that ER localization information is contained in the region between residues 60 and 88 of PIG-L.

The Transmembrane Span of PIG-L Contributes to ER Localization—Our results thus far implicate a stretch of the PIG-L cytoplasmic tail in ER localization of the protein. These results were obtained by analyzing ΔTac-PIG-L chimeras composed of the ecto domain and transmembrane span of Tac and elements of the cytoplasmic tail of PIG-L. These constructs did not test whether the luminal and transmembrane domains of PIG-L contributed to ER localization of the protein. To examine this point we generated constructs $Tac_{ecto}L_{1-26}Tac_{cyto}$ (T-L-T), Tac_{ecto}-L_{1-139}, and Tac_{ecto}-L_{1-43} (Fig. 6*A*). In T-L-T, the luminal and transmembrane domains of PIG-L are inserted in place of the transmembrane domain of Tac. In the constructs Tac_{ecto}-L_{1-139} and Tac_{ecto}-L_{1-43}, the Tac ecto domain is fused to N-terminal portions of PIG-L containing its luminal and transmembrane domains and different lengths of its cytoplasmic tail (up to residues 139 and 43, respectively).

Immunofluorescence microscopy analysis of intact and permeabilized cells expressing T-L-T showed surface labeling as well as significant intracellular staining even in CHX-chased cells (Fig. 6*B*). These results are consistent with SDS-PAGE analyses showing T-L-T both as a high molecular mass, Endo H-resistant glycoprotein as well as an Endo H-sensitive, low molecular mass band (Fig. 6*C*). Quantitation of the SDS-PAGE data indicates that ~70% of T-L-T is in the low molecular mass ER form, whereas ~30% is in the plasma membrane form after a 2.5-h CHX chase. This result suggests that the luminal and transmembrane domains of PIG-L are unable to restrict Tac to the ER, resulting in a significant fraction of the protein being displayed at the cell surface. However, since ~70% of this construct is recovered in low molecular mass form even after a CHX chase (Fig. 6, *C* and *D*), the export of T-L-T from the ER is inefficient. There are a couple of possible explanations for this. First, the luminal and transmembrane domains of PIG-L may contain weak ER retention information that delays ultimate export of T-L-T from the ER. Alternatively, the patchwork nature of the T-L-T construct, unlike the simpler constructs (including the functional ΔTac-L_{26-252} chimera) used for all other experiments in this paper, may impede protein folding and, thus, display delayed export. Similarly, a large fraction of the ER-translocated T-L-T may remain chronically misfolded and is, thus, incapable of escaping the ER quality control system. Analyses of Tac_{ecto}-L_{1-139} and Tac_{ecto}-L_{1-43} (see below) support the first explanation.

Tac_{ecto}-L_{1-139} and Tac_{ecto}-L_{1-43} were both ER localized (Fig. 6, *B* and *C*) even after a 2.5-h CHX chase. The result for Tac_{ecto}-L_{1-139} is anticipated since the ER localization information that we identified in the PIG-L cytoplasmic tail is contained within this construct. However, the ER localization of Tac_{ecto}-L_{1-43} was surprising since a related construct (ΔTac-L_{26-43} (Fig. 5*A*)) lacking the luminal and transmembrane domains of PIG-L is not retained in the ER (Fig. 5, *B* and *C*). Taking this result together with the data on T-L-T presented above, we conclude that the luminal and transmembrane domains of PIG-L contain ER localization information capable of functioning independently of the signal present in the cytoplas-

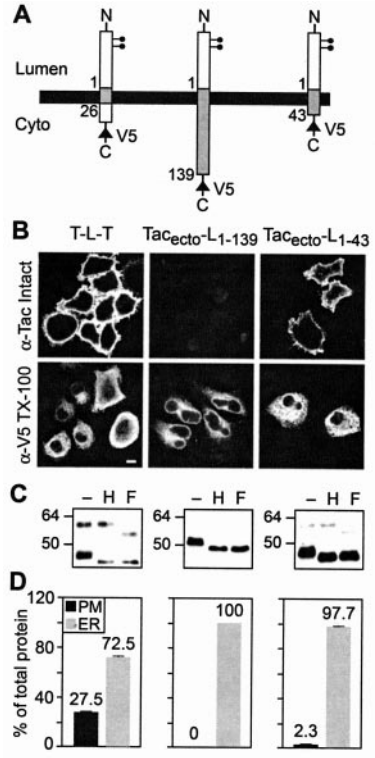

FIG. 6. **The transmembrane domain of PIG-L contributes to its ER localization.** A, schematic illustration of constructs T-L-T, Tac$_{ecto}$-L$_{1–139}$, and Tac$_{ecto}$-L$_{1–43}$. All constructs contain a C-terminal V5 tag. *Cyto*, cytoplasm. *B*, HeLa cells were transfected with cDNAs encoding the various constructs. Two days post-transfection the cells were treated with CHX for 2.5 h before being processed as described in the legend to Fig. 4*B*. *Scale bar*, 5 μm. *C*, the expressed proteins were immunoprecipitated from cell lysates (generated from CHX-treated cells as in *panel B*) and analyzed by glycosidase digestion and SDS-PAGE as described in the legend to Fig. 4*C*. *H*, Endo H; *F*, *N*-glycosidase F. *D*, quantitation of the immunoblots in *panel C* carried out as described in the legend to Fig. 4*D*. *PM*, plasma membrane.

mic tail of the protein and that the presence of membrane proximal residues of the cytoplasmic domain augments the retention activity of the luminal and transmembrane domains.

DISCUSSION

Our data show that both PIG-L protein and GlcNAc-PI de-*N*-acetylase activity are equally concentrated in ER and MAM fractions derived from HeLa cells. This result contrasts with previous data generated by us and by others in which subcellular fractionation of mouse thymoma cells yielded a distinct microsomal fraction enriched in GlcNAc-PI de-*N*-acetylase activity (8, 12). In these previous studies we identified the GlcNAc-PI de-*N*-acetylase-enriched mouse thymoma fraction as MAM because of the method used for its isolation (identical to the scheme shown in Fig. 2*A*) as well as its characteristically lower specific activity of NADPH cytochrome *c* reductase relative to traditionally isolated ER (identical to the data shown for HeLa MAM in Fig. 2*B*) (8). We suggest that the difference in results obtained with mouse thymoma *versus* HeLa cells can be attributed to the subtle, cell type-specific variation in subcellular compartmentation that is seen in many systems. For example, a similar cell type-specific variation in ER *versus* MAM distribution has been documented for an isoform of phosphatidylethanolamine *N*-methyltransferase (PEMT-2), an enzyme that is uniquely localized to MAM in rat liver subcellular fractions but is distributed uniformly between MAM and ER fractions derived from human liver (29). Other examples of proteins whose fine subcellular location depends on cell type include the α-mannosidases I and II (30) and the terminal glycosyltransferases α1,3-*N*-acetyl-galactosaminyltransferase (31) and α2,6-sialyltransferase (31, 32); these enzymes occupy different regions of the Golgi stack depending on cell type.

We present data showing that PIG-L is an ER-localized type I membrane protein. The addition of *N*-glycosylation sites to PIG-L as in the functional Tac-PIG-L chimeras Tac$_{ecto}$-L or ΔTac-L$_{26–252}$ (Fig. 4) or in the ANSTS-FLAG-PIG-L-GFP construct (Fig. 3*B*) results in ER-localized proteins with Endo H-sensitive *N*-glycans. Because the *N*-glycans in these proteins do not undergo any detectable Golgi-specific modifications even in CHX-chased cells (although they do become Endo H-resistant if the PIG-L sequence in the chimera is truncated severely enough to allow the protein to exit the ER (Fig. 5)), it is clear that PIG-L does not cycle through the Golgi to a detectable extent (19) and may be directly retained in the ER. Our data indicate that this "retention" is mediated by sequence determinants located between amino acids 60 and 88 in the cytoplasmic tail of PIG-L as well as by the luminal and transmembrane domains of the protein.

PIG-L cytoplasmic sequences containing residues 60–88 are sufficient to retain a ΔTac-PIG-L chimera in the ER (Fig. 5). ClustalW multiple sequence alignment (33) of PIG-L orthologs highlights a stretch of cytoplasmic sequence between residues 60 and 88 of human PIG-L (^{64}**L**ARLRHW<u>V</u>Y<u>LL</u>**C**^{75}<u>F</u>**S**^{77}**AG**^{79}) containing four amino acid residues (shown in bold) that are conserved among all PIG-L species as well as a conserved hydrophobic patch (underlined) that could potentially mediate protein-protein or protein-membrane interactions. Thus the hydrophobic stretch may interact with the lipid bilayer, possibly by penetrating the bilayer as a shallow hairpin confined weakly to the cytoplasmic leaflet of the ER membrane. Such an interaction has been suggested for cytochrome P450, an ER-localized type I membrane protein with two hydrophobic patches in its cytoplasmic tail (34, 35). In addition, the conserved cysteine residue (Cys-75) may be thioacylated (36), promoting membrane association. These putative interactions between a cytoplasmic domain of PIG-L and the membrane may serve to segregate the protein into a domain that prevents it from accessing ER exit sites. An alternative possibility concerns the propensity of short hydrophobic sequences to promote protein-protein interactions. It is known that short hydrophobic patches arranged in a β-sheet conformation can cause multimerization. An example of this is the pentapeptide sequence KLVFF that is responsible for polymerization of the Alzheimer's amyloid β-peptide into amyloid fibrils (37). Interestingly, preliminary velocity gradient sedimentation analyses indicate that while SDS-extracted FLAG-PIG-L-V5 sediments at <3.6 S, consistent with its ~32-kDa monomeric size, Nonidet P-40-extracted protein sediments at ~4.2 S, similar to a bovine serum albumin standard (~66 kDa) (data not shown). This result suggests that FLAG-PIG-L-V5 exists as a dimer or slightly larger complex in Nonidet P-40 extracts or that it interacts with another protein of similar size. It is possible that larger, labile complexes exist *in situ* that are pared down to dimeric size on Nonidet P-40 extraction. Nevertheless, either multimer or dimer formation or a heterologous interaction, possibly mediated by the hydrophobic patch in concert with or independently of contributions from the transmembrane span (see below), could be the basis of PIG-L retention in the ER. Multimerization could physically restrict a PIG-L aggregate from entering a transport vesicle bud or, through multivalency, promote the interaction between PIG-L and other ER-associated molecules and so prevent export. More work needs to be done to sort out these ideas and to delineate aspects of the

sequence between residues 60 and 88 that are critical in signaling ER retention.

Our data indicate that the transmembrane span of PIG-L, although unable to act as a strong retention signal in the context of the T-L-T construct (Fig. 6), is clearly able to retain Tac_{ecto}-L_{1-43}, a chimera that lacks the cytoplasmic retention signal discussed above. We conclude that the transmembrane domain contributes independent ER localization information when placed in the context of membrane proximal residues of the cytoplasmic domain that lack any retention information. Although the sequence of the transmembrane domain of PIG-L offers no clues as to how this region might mediate ER localization, there are many precedents for transmembrane domains of membrane proteins contributing organellar localization information through their ability to promote multimerization. Examples include Golgi-localized enzymes (*e.g.* α2,6-sialyltransferase (38–40)), Golgi-targeted viral glycoproteins (*e.g.* E1 glycoprotein of avian *Coronavirus* (41, 42)), and the intermediate compartment protein CLIMP-63 (43) as well as ER membrane proteins such as ribophorin II (44) and cytochrome P450 (34, 45). In the latter cases the transmembrane domain represents only one component of a multicomponent retention signal, with other domains of the protein contributing to localization information as well. In the case of ribophorin II, a type I membrane protein, it was shown that although the luminal domain does not contain a detectable independent retention signal, it augments the retention activity of the transmembrane domain (44). Similarly, in cytochrome P450 2C1, three amino acids immediately after the transmembrane domain were found to be critical for exclusion of the protein from ER transport vesicles (46). As suggested for these enzymes, it is possible that a short cytoplasmic region may serve to properly position the transmembrane domain within the lipid bilayer of the ER, thus enhancing the potency of its retention signal. The context-dependent nature of the transmembrane domain retention signal in ER-localized Tac_{ecto}-L_{1-43} *versus* cell surface expressed T-L-T suggests that it is not the length of the transmembrane domain which is critical for its retention function. The length of the transmembrane domain has been suggested as a characteristic distinguishing ER, Golgi, and plasma membrane proteins because of the differing cholesterol content of these membranes and the resulting variation in bilayer thickness (39, 40, 47).

In conclusion, our results indicate that PIG-L is retained in the ER by two retention signals, an independent signal, located in its cytoplasmic domain, and a second signal in its transmembrane domain that is functional in the presence of membrane proximal residues of the cytoplasmic tail. Although it is unclear how these signals work to retain PIG-L in the ER, we favor a model in which PIG-L is denied access to ER exit sites or vesicle buds through a segregation mechanism involving multimerization, interaction with other ER-associated proteins, or an interaction between its cytoplasmic domain and the membrane. Regardless of the precise mechanism, our findings add another protein to the list of already characterized, ER, and intermediate compartment-localized proteins like ribophorin II, cytochrome P450, and CLIMP-63 that contain multiple localization signals.

Acknowledgments—We thank Karen Colley, Becky Montgomery, Chris Nicchitta, Vicky Stevens, Saulius Vainauskas, and Thomas Waldmann for reagents and cell lines, Saulius Vainauskas and Jolanta Vidugiriene for technical advice, Steve Fuchs and Ron Raines for discussion, Laura van der Ploeg for preparing the figures, Sara Crittenden for instructions on the use of the Kimble lab confocal microscope, the Martin lab for use of an electroporator for initial experiments, the University of Wisconsin flow lab staff for help with flow cytometry, and Sandy Harding, Weng-Chi Man, and Mari Nojiri for comments on the manuscript. A. K. M. acknowledges Bob Dylan and Alec Leamas (assistant librarian) for stimulation.

REFERENCES

1. Kinoshita, T., and Inoue, N. (2000) *Curr. Opin. Chem. Biol.* **4,** 632–638
2. McConville, M. J., and Menon, A. K. (2000) *Mol. Memb. Biol.* **17,** 1–16
3. Tiede, A., Bastisch, I., Schubert, J., Orlean, P., and Schmidt, R. E. (1999) *Biol. Chem.* **380,** 503–523
4. Eisenhaber, B., Maurer-Stroh, S., Novatchkova, M., Schneider, G., and Eisenhaber, F. (2003) *BioEssays* **25,** 367–385
5. Vidugiriene, J., and Menon, A. K. (1993) *J. Cell Biol.* **121,** 987–996
6. Vidugiriene, J., and Menon, A. K. (1994) *J. Cell Biol.* **127,** 333–341
7. Murakami, Y., Siripanyapinyo, U., Hong, Y., Kang, J. Y., Ishihara, S., Nakamuna, H., Maeda, Y., and Kinoshita, T. (2003) *Mol. Biol. Cell* **14,** 4285–4295
8. Vidugiriene, J., Sharma, D. K., Smith, T. K., Baumann, N. A., and Menon, A. K. (1999) *J. Biol. Chem.* **274,** 15203–15212
9. Vance, J. E. (1990) *J. Biol. Chem.* **265,** 7248–7256
10. Lewis, J. A., and Tata, J. R. (1973) *J. Cell Sci.* **13,** 447–459
11. Meier, P. J., Spycher, M. A., and Meyer, U. A. (1981) *Biochim. Biophys. Acta* **646,** 283–297
12. Stevens, V. L., Zhang, H., and Kristyanne, E. S. (1999) *Biochem. J.* **341,** 577–584
13. Nakamura, N., Inoue, N., Watanabe, R., Takahashi, M., Takeda, J., Stevens, V. L., and Kinoshita, T. (1997) *J. Biol. Chem.* **272,** 15824–15840
14. Watanabe, R., Ohishi, K., Maeda, Y., Nakamura, N., and Kinoshita, T. (1999) *Biochem. J.* **339,** 185–192
15. Stevens, V. L., Zhang, H., and Harreman, M. (1996) *J. Biochem.* **313,** 253–258
16. Smith, T. K., Sharma, D. K., Crossman, A., Dix, A., Brimacombe, J. S., and Ferguson, M. A. J. (1997) *EMBO J.* **16,** 6667–6675
17. Sharma, D. K., Smith, T. K., Weller, C. T., Crossman, A., Brimacombe, J. S., and Ferguson, M. A. J. (1999) *Glycobiology* **9,** 415–422
18. Smith, T. K., Crossman, A., Borrissow, C. N., Peterson, M. J., Dix, A., Brimacombe, J. S., and Ferguson, M. A. J. (2001) *EMBO J.* **13,** 3322–3332
19. Teasdale, R. D., and Jackson, M. R. (1996) *Annu. Rev. Cell Dev. Biol.* **12,** 27–54
20. Vainauskas, S., Maeda, Y., Kurniawan, H., Kinoshita, T., and Menon, A. K. (2002) *J. Biol. Chem.* **277,** 30535–30542
21. Vainauskas, S., and Menon, A. K. (2004) *J. Biol. Chem.* **279,** 6540–6545
22. Baumann, N. A., Vidugiriene, J., Machamer, C. E., and Menon, A. K. (2000) *J. Biol. Chem.* **275,** 7378–7389
23. Leonard, W. J., Depper, J. M., Crabtree, G. R., Rudikoff, S., Pumphrey, J., Robb, R. J., Krönke, M., Svetlik, P. B., Peffer, N. J., Waldmann, T. A., and Greene, W. C. (1984) *Nature* **311,** 626–631
24. Bonifacino, J. S., Suzuki, C. K., and Klausner, R. D. (1990) *Science* **247,** 79–82
25. Horton, R., Hunt, H., Ho, S., Pullen, J., and Pease, L. (1989) *Gene* (*Amst.*) **77,** 61–68
26. Stone, S. J., and Vance, J. E. (2000) *J. Biol. Chem.* **275,** 34534–34540
27. Cui, Z., Vance, J. E., Chen, M. H., Voelker, D. R., and Vance, D. E (1993) *J. Biol. Chem.* **268,** 16655–16663
28. Stornaiuolo, M., Lotti, L. V., Borgese, N., Torrisi, M.-R., Mottola, G., Martire, G., and Bonatti, S. (2003) *Mol. Biol. Cell* **14,** 889–902
29. Shields, D. J., Lehner, R., Agellon, L. B., and Vance, D. E (2003) *J. Biol. Chem.* **278,** 2956–2962
30. Velasco, A., Hendricks, L., Moreman, K. W., Tulsiani, D. R. P., Touster, O., and Farquhar, M. G. (1993) *J. Cell Biol.* **122,** 39–51
31. Roth, J., Taatjes, D. J., Weinstein, J., Paulson, J. C., Greenwell, P., and Watkins, W. M. (1986) *J. Biol. Chem.* **261,** 14307–14312
32. Roth, J., Taatjes, D. J., Lucocq, J. M., Weinstein, J., and Paulson, J. C. (1985) *Cell* **43,** 287–295
33. Combet, C., Blanchet, C., Geourjon, C., and Deléage, G. (2000) *Trends Biochem. Sci.* **25,** 147–150
34. Szczesna-Skorupa, Ahn, K., Chen, C.,- D., Doray, B., and Kemper, B. (1995) *J. Biol. Chem.* **270,** 24327–24333
35. Ohta, Y., Kawato, S., Tagashira, H., Takemori, S., and Kominami, S. (1992) *Biochemistry* **31,** 12680–12687
36. Linder, M. E., and Deschenes, R. J. (2003) *Biochemistry* **42,** 4311–4320
37. Tjernberg, L. O., Näslund, J., Lindqvist, F., Johansson, A. R., Karlström, A. R., Thyberg, J., Terenius, L., and Nordstedt, C. (1996) *J. Biol. Chem.* **271,** 8545–8548
38. Aoki, D., Lee, N., Yamaguchi, N., Dubois, C., and Fukuda, M. N. (1992) *Prot. Natl. Acad. Sci. U. S. A.* **89,** 4319–4323
39. Munro, S. (1995) *EMBO J.* **14,** 4695–4704
40. Colley, K. J. (1997) *Glycobiology* **7,** 1–13
41. Swift, A. M., and Machamer, C. E. (1991) *J. Cell Biol.* **115,** 19–30
42. Machamer, C. E. (1991) *Curr. Opin. Cell Biol.* **5,** 606–612
43. Schweizer, A., Rohrer, J., Hauri, H.-P., and Kornfeld, S. (1994) *J. Cell Biol.* **126,** 25–39
44. Fu, J., Pirozzi, G., Sanjay, A., Levy, R., Chen, Y., Lemos-Chiarandini, C. D., Sabatini, D. D., and Kreibich, G. (2000) *Eur. J. Cell Biol.* **79,** 219–228
45. Szczesna-Skorupa, E., and Kemper, B. (2000) *J. Biol. Chem.* **275,** 19409–19415
46. Szczesna-Skorupa, E., and Kemper, B. (2001) *J. Biol. Chem.* **276,** 45009–45014
47. Bretscher, M. S., and Munro, S. (1993) *Science* **261,** 1280–1281